Received: 17 October 2022 | Revised: 12 February 2023 | Accepted: 14 February 2023

DOI: 10.1002/asl.1161

RESEARCH ARTICLE

Atmospheric Science Letters RMetS

A spatiotemporal analysis of precipitation anomalies using rainfall Gini index between 1980 and 2022

Ghada Sahbeni[1,2] | **Jean Baptiste Pleynet**[2] | **Konrad Jarocki**[2]

[1]Department of Geophysics and Space Science, Eötvös Loránd University, Budapest, Hungary

[2]IBISA SA, Luxembourg, Luxembourg

Correspondence
Ghada Sahbeni, Department of Geophysics and Space Science, Eötvös Loránd University, Budapest, Pázmány Péter Stny, 1/C, 1117, Hungary.
Email: gsahbeni@caesar.elte.hu

Abstract

As a reaction to the expanding challenges associated with social susceptibility and their interconnection to diverse environmental threats, parametric insurance plays a key role as an innovation tool in the insurance sector to enhance social resilience to natural disasters and extreme climatic conditions, which can tremendously impact several economic sectors, including agriculture and as a result food security. In this context, this research investigates the association between rainfall Gini index and drought events in Western Europe. For this purpose, we acquired ERA5 data for daily precipitation for five locations from 1980 to 2022. Gini index (GI) values were calculated and analyzed for each location with the Mann–Kendall test at a 5% significance level. As expected, a minimal decreasing trend has been observed for daily precipitation, while an increasing trend was recorded for Gini index. In addition, data on the soil moisture index (SMI) and top drought events were extracted from the European Drought Observatory (EDO) to explore their potential connection with the Gini index over time and space. Although a moderately low to negligible correlation, ranging between −0.27 and 0.02, was found between SMI and GI, a qualitative comparison between major drought episodes and Gini index anomaly showed that similar spatiotemporal patterns are present across the region, particularly for extreme drought events in 1996–1997 and 2003. The current study elucidates the rainfall Gini index's efficiency as a drought indicator for qualitative analysis, yet more work must be conducted to quantitatively evaluate its association with drought magnitude.

KEYWORDS

daily precipitation, drought, ERA5, rainfall Gini index, soil moisture index

1 | INTRODUCTION

For many hydro-climatological investigations, precipitation is a crucial meteorological metric to determine regional and global climate change risks (Soltani et al., 2016). As a matter of fact, precipitation depicts a primary hydrologic factor in the land surface water balance, where it replenishes soil moisture, supports vegetation growth, and maintains surface flows and groundwater resources, linking atmospheric and land

surface processes together (Abed-Elmdoust et al., 2016; Alimonti et al., 2022; Sarker et al., 2019). Therefore, assessing precipitation patterns and distribution is an essential task toward mitigating the impacts of climate change and improving resilience to extreme weather events and natural disasters. By improving our understanding of precipitation patterns and distribution, we can develop better tools and strategies for managing water resources and reducing drought risks.

Precipitation anomalies induced by climate change tremendously influence crop yield and environmental sustainability, which affect food security worldwide (Zaveri et al., 2020). As a result, understanding its significant impacts on agricultural productivity has recently become crucial as climate change accelerates, although rainfall anomalies have proven to be a severe barrier to human civilization for centuries (Coughlan de Perez et al., 2019; Singh et al., 2018). Changes in daily precipitation distribution have already been picked up in observational records, given that global warming reached 1.5°C in 2022 (IPCC, 2022). For instance, an observational study by Rajah et al. (2014) found global trends in extreme and light precipitation events between 1976 and 2000 using data from 12,513 ground-based stations. Similarly, several regional studies have detected changes in precipitation frequency in Europe and worldwide (Masson-Delmotte et al., 2005; Zeder & Fischer, 2020; Huo et al., 2021), which could be associated with climate change.

As a result of severe climate change, extreme drought events are expected to increase in both frequency and magnitude (Seneviratne et al., 2021), potentially necessitating the incorporation of suitable parametric insurance strategies to mitigate its financial impacts on agricultural production, allowing farmers to recover from the disaster at a faster pace (Broberg, 2019). Parametric insurance is a tool for reducing drought impacts in agriculture, serving as a self-sufficient mitigation mechanism to attenuate social vulnerability to environmental disasters from a broad perspective (Radu & Alexandru, 2022). Typically, it is based on robust indices that have been demonstrated to be correlated with natural disasters (Monteleone et al., 2020), such as drought. Incidentally, the Gini index concept for evaluating rainfall inequalities over a defined period has been used in climate change-related studies (Sangüesa et al., 2018; Voskresenskaya et al., 2013); however, no research has been conducted to study its potential association with drought on the regional scale. Therefore, this research examines daily precipitation changes in five locations in Western Europe between 1980 and 2022. Once precipitation trends and the rainfall Gini index were determined, a correlation analysis was conducted to explore the association between soil moisture index (SMI) and precipitation anomalies between 1995 and 2019. In the present study, Europe's top drought events during the past 42 years have been investigated and linked with the rainfall Gini index anomaly to comprehend its efficiency as a drought indicator for qualitative assessment.

2 | DATA AND METHODS

2.1 | Daily precipitation data

ERA5 provides hourly estimates of many atmospheric, land, and oceanic climate variables produced by the European Center for Medium-Range Weather Forecasts (ECMWF) in the Copernicus Climate Change Service framework (C3S, 2022. Data encompass the planet on a grid of 30·km, using 137 levels to characterize the atmosphere from the ground up to an 80·km altitude. Reduced spatial and temporal resolution information for all variables is included in ERA5 data (Hersbach et al., 2019; Hersbach, Bell, Berrisford, Dahlgren, et al., 2020). Monthly updates of ERA5 from 1959 to the present are provided in real-time within 3 months, while the preliminary daily updates are available within 5·days (Hersbach, Bell, Berrisford, Hirahara, et al., 2020). More detailed information about the ERA5 data can be found in ECMWF (2022) documentation. This analysis was conducted from 1980 to 2022 for five locations in Eastern France, as illustrated in Figure 1, with an average record length of 42 years. This period was chosen because precipitation is highly variable and depends not only on climate type and geography (Ghorbani et al., 2021) but also on large-scale weather patterns, which require several years to be assessed (Ali et al., 2003). Moreover, it is the most prolonged period of well-represented ERA5 data compared to the period between 1959 and 1979, as stated in the Climate Data Guide (2022).

2.2 | Gini index concept

Gini index, which ranges between zero and one, with zero indicating a uniform distribution of precipitation across all days within a year while one indicating precipitation anomalies, offers a measure of how uneven rainfall is distributed over a period of time (Duan et al., 2022). Before that, it was initially developed by the Italian statistician Corrado Gini in 1912 and adopted for economics to assess wealth disparity (Ceriani & Verme, 2012), but more recently, it has been proposed in other scientific fields like hydrology (e.g., Masaki et al., 2014) and geology (e.g., Edgar et al., 2020). As variability parameters,

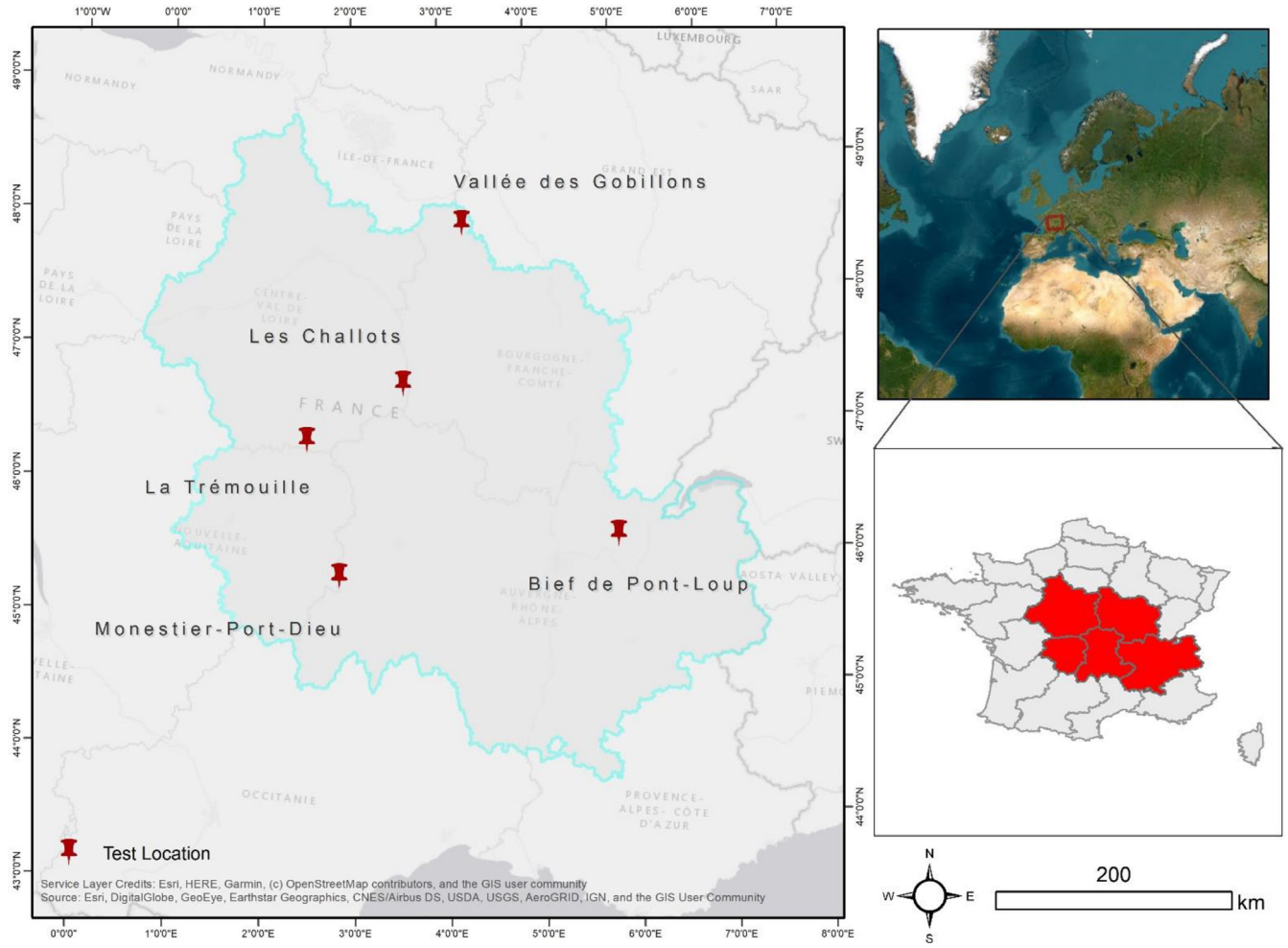

FIGURE 1 Geographic location of the selected test plots.

like standard deviation and variance, are sensitive to the scale and probability of data distribution, the Gini index is more robust and nondimensional, making it less complicated to use under diverse scenarios (Monjo & Martín-Vide, 2016).

Once daily precipitation is acquired, cumulatively aggregated, and normalized to a proportion of total precipitation, the Lorenz curve, a graphical representation of inequality degree in data distribution, is used to determine the Gini index value (Gastwirth, 1972). The Gini index is obtained by multiplying the region between the Lorenz curve and the 45° line by two, representing a uniform precipitation distribution, as expressed in Equation (1).

$$G = \frac{1}{n}\left(n + 1 - 2\left(\frac{\sum_{i=1}^{n}(n+1-i)y_i}{\sum_{i=1}^{n} y_i}\right)\right) \quad (1)$$

where G is the Gini index, n is the total number of days, and y_i is the precipitation for the ith day.

A spatiotemporal analysis of Gini index results showed that the index is susceptible to wet days number in a given year (Sangüesa et al., 2018). Therefore, the relationship between the Gini index and SMI was evaluated using Pearson Correlation via RStudio. Moreover, Gini index distribution was compared with drought events, expecting a connection between drought and high Gini index values. To account for limited data availability, the consistency of the results was assessed using two time periods: the SMI spanning from 1995 to 2019 and the most significant drought events occurring between 1980 and 2016.

2.3 | Temporal trend in daily precipitation and Gini index

Before assessing the temporal trend in daily precipitation data, we checked for autocorrelation in time series data, which is crucial as it can affect the accuracy of statistical inference. Autocorrelation occurs when time series

values at a given point in time are related to their past values. This can result in nonindependence between observations, which can cause problems in estimating statistical models and calculating hypothesis tests. Therefore, we used the autocorrelation function (ACF) within the "stats" package in RStudio. Based on the test results, it can be concluded that there is no significant autocorrelation in the data since the autocorrelation coefficient ranged on average between −0.005 and −0.02 at a 5% significance level. Then, the Mann–Kendall statistical test was used at all five locations to evaluate trends in daily precipitation and the Gini index at a 5% significance level. The nonparametric test does not presume anything about the data's marginal probability distribution, ascertaining data independency to time (Sangüesa et al., 2018; Song et al., 2015). The Mann–Kendall Trend test's fundamental principle is to compare the signs of earlier and later data points. Therefore, if a trend is present, the sign values will continuously increase or decrease (Meals et al., 2011). Detailed information about the test can be found in Karmeshu (2012) and Wang et al. (2020).

Khambhammettu (2005) claims that the data values are assessed as an ordered time series. All following data values are compared to each value. The Mann–Kendall statistic, S, is initially assumed to have a value of zero, then increased by one if a data value from a later period is more significant than a data value from an earlier period, and vice versa. The final value of S is the sum of all increments and decrements.

Given data points x_1, x_2, ... x_n, x_j represents the data point at time j. The Mann–Kendall statistic (S) is determined by Equation (2).

$$S = \sum_{k=1}^{n-1} \sum_{j=k+1}^{n} sign\left(x_j - x_k\right) \tag{2}$$

where:

$$sign\left(x_j - x_k\right) = 1 \; if \; x_j - x_k > 0$$

$$= 0 \; if \; x_j - x_k = 0$$

$$= -1 \; if \; x_i - x_k < 0$$

A positive value of S suggests an upward trend, whereas a negative value indicates a downward trend. The probability associated with S and the sample size n must be determined to assess the trend significance statistically.

Then, the variance VAR(S) is determined, as expressed in Equation (3).

$$\mathrm{VAR}(S) = \frac{1}{18}\left[n(n-1)(2n+5) - \sum_{p=1}^{q} t_p\left(t_p - 1\right)\left(2t_p + 5\right)\right] \tag{3}$$

Finally, the Z value is calculated depending on S and its variance.

$$Z = \frac{S-1}{\sqrt{VAR(S)}}; if \; S > 0$$

$$Z = 0; if \; S = 0$$

$$Z = \frac{S+1}{\sqrt{VAR(S)}}; if \; S < 0 \tag{4}$$

2.4 | Soil moisture index

Along with precipitation and evapotranspiration, soil moisture is a key factor in plant growth and a fundamental part of the hydrological cycle. The SMI is defined as the ratio of the difference between present soil moisture and the permanent wilting point to field capacity and residual soil moisture (SMI). A score of zero indicates arid conditions, whereas a score of one indicates extremely wet conditions (Saha et al., 2018; Zhang et al., 2017). The Copernicus European Drought Observatory (EDO) uses SMI to track the beginning and end of agricultural drought conditions, which appear when soil moisture availability to plants falls; hence adversely affects crop output and, consequently, agricultural productivity (Cammalleri et al., 2016). The SMI retrieved from EDO is produced by the joint research center (JRC) using LISFLOOD hydrological model with a spatial resolution of 5·km (Van Der Knijff et al., 2010) relative to a climatological reference period (1995–2022) (De Roo et al., 2000). The drought indicator assesses one of the three primary droughts—agricultural drought—based on the hydrological cycle variables (Laguardia & Niemeyer, 2008). Agricultural drought results in decreased crop production due to insufficient soil moisture, while hydrological drought is characterized by below-average water availability in rivers, streams, reservoirs, lakes, or groundwater, and both droughts are typically preceded by a meteorological drought, which is a prolonged period of less than average rainfall in a given region. More details about SMI can be found in the EDO indicator factsheet (EDO, 2021).

SMI is determined using Equation (5), with θ being the daily soil moisture and θ_{50} being the average between the wilting point and the field capacity.

$$\mathrm{SMI} = 1 - \frac{1}{1 + \left(\frac{\theta}{\theta_{50}}\right)^6} \quad (5)$$

We did not normalize SMI as suggested by a few studies (e.g., Grillakis (2019)) to maintain its seasonal representation, as SMI is merely a measure of soil moisture, reflecting the seasonal patterns of precipitation and evapotranspiration. Therefore, removing the inherent seasonality would fundamentally change the significance of the SMI and may not accurately reflect the underlying dynamics of the soil moisture system, in other words, to preserve the temporal patterns since seasonality is a critical factor in the water cycle and influences the temporal variability of moisture. Modifying the SMI by removing the latter may mask significant temporal signals related to precipitation and evapotranspiration, which are crucial to characterizing the water cycle and monitoring drought conditions.

2.5 | Top drought events database

The Global Drought Observatory provides free access to its drought events database, which was compiled by Spinoni et al. (2019) using over 4500 global drought events that occurred between 1951 and 2016. At various temporal scales, they have been categorized using a few metrics, including the standardized precipitation index (SPI) (McKee et al., 1993) and the standardized precipitation evapotranspiration index (SPEI) (Vicente-Serrano et al., 2010), which are the most commonly used multiscalar indicators based on climatic data to determine meteorological droughts. Even though the standardized precipitation evapotranspiration index (SPEI) is a refined version of the widely used standardized precipitation index (SPI), it has the advantage of considering not only precipitation but potential evapotranspiration (PET) when evaluating drought. A detailed description of SPI and SPEI can be found in EDO's indicator factsheet (2021).

The database contains separate entries for around 175 countries and macroregions on a spatial scale; among them, 52 of the largest mega-droughts occurred between 1951 and 2016 using a specific classification scoring system (Spinoni et al., 2019). Moreover, according to the database, Amazonia, southern South America, the Mediterranean region, much of Africa, and north-eastern China stand out as drought hotspots. With rising temperatures over North America, Central Europe, Central Asia, and Australia, precipitation anomalies increased, leading to frequently severe droughts, which will be investigated in this study.

The drought events database is updated every 2·years and serves as a valuable resource for both scientific investigations and policy reports. This study has incorporated the database to compare drought patterns between 1980 and 2016 with the spatiotemporal distribution of the Gini index in the selected region. Further, this study aims to qualitatively examine the interconnection between yearly precipitation inequality and the probability of a drought event occurring in the same year.

3 | RESULTS AND DISCUSSION

3.1 | Descriptive analysis

Table 1 illustrates the main statistical parameters for daily precipitation in selected locations over the last 42·years. From 1980 to 2022, significant increases and decreases in rainfall distribution were recorded. The distribution of daily precipitation values is characterized by a significant difference between the minimum and maximum values, reflecting this parameter's spatial variability. Further, a discard between the mean and median values has been observed for all locations, revealing a positive skewness in time-series data. Minimal decreasing trends were predominantly observed with a tau value ranging between −0.259 and −0.256 at a 5% significance level. This decreasing trend is mainly consistent with the European Environment Agency report published in 2017 (EEA, 2017), which revealed a decreasing trend in annual precipitation across western and southern Europe between 1960 and 2015.

The main statistical parameters for the Gini index are given in Table 2. A slight difference between the minimum and maximum values was observed, indicating a spatial variability of the Gini index over time. Plus, the normality test demonstrated that the index is normally distributed with a remarkably close range between mean and median values. The coefficient of variation (CV), which is a relative measure of data distribution expressed as the fraction of standard deviation to mean, ranged between 3.36% and 3.69% for all test locations, revealing the consistency and reliability of measured values. The CV can help compare variation degrees from one dataset to another, which was insignificant in this case. Based on Table 2 and Figure 2, increasing trends were observed in Gini index variation over time for test locations, with a tau value ranging between 0.18 and 0.3 at a 5% significance level. The positive trend is somehow in agreement with Rajah et al. (2014), who discovered a significantly decreasing frequency of wet days in the same region between 1976 and 2000. Given that the Gini index is a direct indicator of rainfall distribution inequality over time, this change in frequency has led to a positive trend.

Test area	Daily precipitation (mm)			
	Minimum	Maximum	Mean	Median
Monestier-Port-Dieu	0	57.1	3.31	0.76
Bief de Pont-Loup	0	95.01	2.95	0.21
La Trémouille	0	54.23	2.57	0.61
Les Challots	0	46.2	2.47	0.48
Vallée des Gobillons	0	50	2.33	0.47

TABLE 1 Daily precipitation variation from 1980 to 2022 in selected locations.

Test area	Gini index					
	Min	Max	Mean	Median	CV (%)	Tau
Monestier-Port-Dieu	0.67	0.77	0.72	0.72	3.62	0.18
Bief de Pont-Loup	0.74	0.84	0.78	0.78	3.36	0.23
La Trémouille	0.68	0.77	0.72	0.72	3.4	0.21
Les Challots	0.69	0.79	0.74	0.74	3.69	0.25
Vallée des Gobillons	0.68	0.82	0.74	0.73	3.62	0.3

TABLE 2 Descriptive statistics of Gini index time-series data for different test areas.

3.2 | SMI and GI

Using RStudio, a Pearson correlation between SMI anomaly values and the Gini index for each station was separately conducted to evaluate precipitation anomalies' effect on soil moisture. Correlation between the GI and SMI anomaly retrieved from the EDO portal shows a negligible to moderately low correlation varying between −0.27 and 0.02, as illustrated in Figure 3. To some extent, the correlation was expected to be moderately negative, which occurred only in two locations (i.e., Monestier-Port-Dieu and Les Challots). Since soil moisture patterns depend not only on precipitation variability but also on evapotranspiration and runoff (McCabe & Wolock, 2013), connections between soil moisture as a feedback mechanism for precipitation and other processes are not simply linear; hence soil moisture dependency on precipitation among other hydrologic components is to be studied (Liang et al., 2010). Further, soil moisture is affected by other pedogenic factors like soil texture, composition, and organic matter content, as well as geomorphic and topographic properties like land cover and altitude, which agrees with Sehler et al. (2019), who investigated the complex relationship between soil moisture and precipitation using remote sensing data. The study found that soil moisture and precipitation have a higher correlation under sparse vegetated dry areas, whereas forests and densely vegetated regions have a weaker relationship, which is the case of selected locations, as illustrated in Figure 1.

Although the correlation between SMI anomaly and Gini index is extremely low, a qualitative analysis of graphs presented in Figure 4 revealed a sort of synchrony, to some extent, between Gini index and SMI anomalies. Over time, variations in SMI anomaly coincide with a rise in Gini index anomaly resulting in a local maximum. For instance, a peak in GI anomaly at Monestier-Port-Dieu in 1998, 2000, 2004, and 2013 is synchronized or shortly followed by a gradual change in SMI anomaly. This is even more prominent in these stations, that is, Bief de Pont-Loup, Les Challots, and Vallée des Gobillons, for the same period. The contemporaneous nature of this phenomenon may be attributed to the complex interactions between the various components of the hydrological cycle, spanning from the atmosphere to the soil, across both space and time. These findings align with previous research by Meng et al. (2018) and Wang et al. (2018). However, it is essential to note that these interpretations are solely based on present observations, and further research can be carried out to explore this aspect in greater detail.

While SMI can be a reliable index for assessing drought events, it has a few limitations to be considered when interpreting its values and integrating it into decision-making regarding resource management and planning. SMI only provides information about the moisture content of the soil's top layer and does not consider the deeper layers, which can also be essential for agricultural and ecosystem processes (Dai & Trenberth, 2004). In addition, it is often calculated using remote sensing data, which can have limitations in terms of spatiotemporal resolution (Schwank et al., 2013). For instance, remote sensing data may not accurately reflect the spatial variability of soil moisture within a given area, as it can be easily affected by

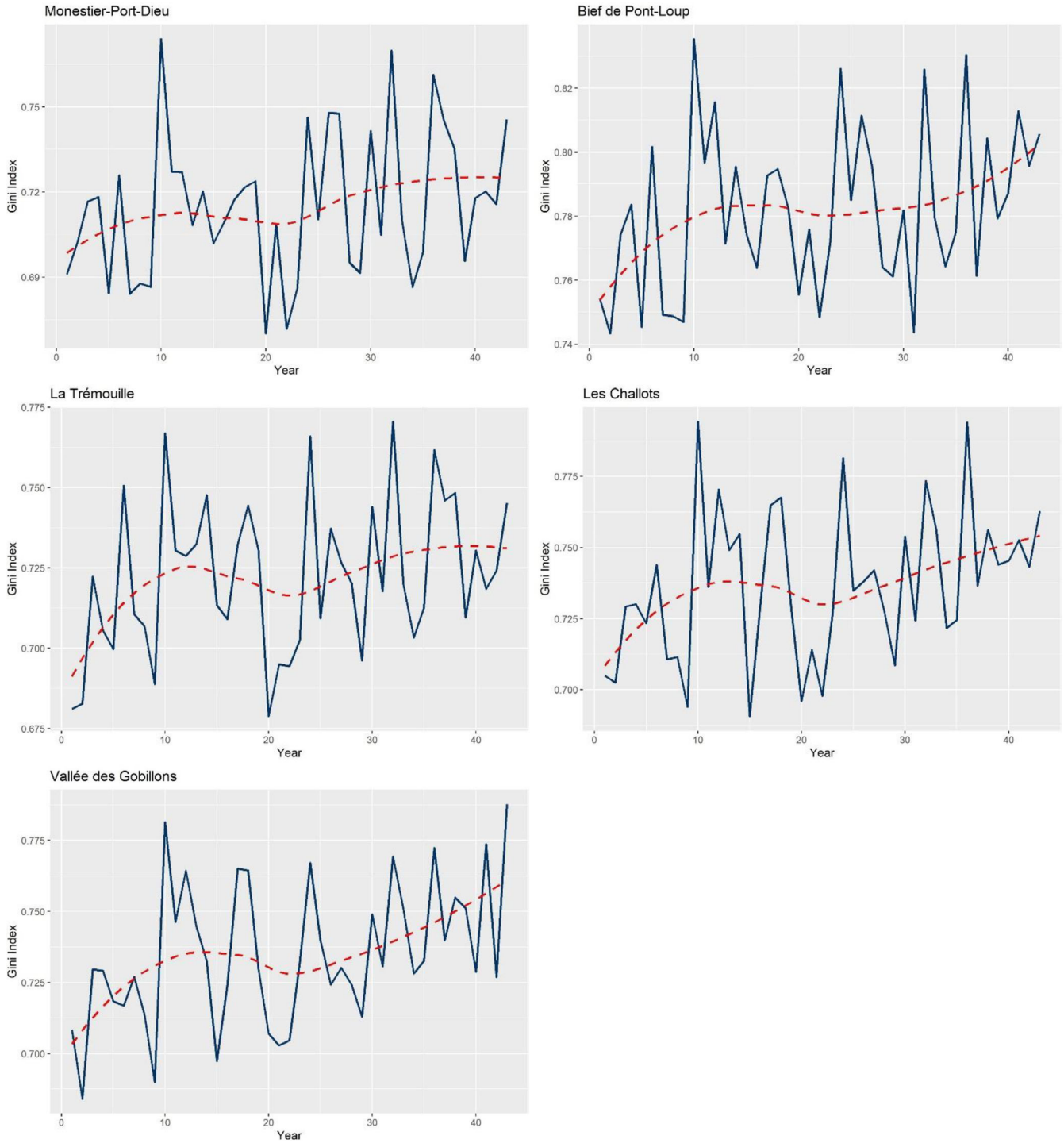

FIGURE 2 The temporal trend of the rainfall Gini index in the test locations based on the Kendall–Mann test over 42·years.

vegetation cover, atmospheric conditions, and the presence of wet surfaces (Jackson et al., 2010).

3.3 | Top drought events and Gini index

As a severe natural hazard, drought has occurred in diverse macroregions from arid to subhumid climates (Carrão et al., 2016). This has attracted researchers' attention to study its spatial distribution, origins, and impacts in order to mitigate its risks (Mishra & Singh, 2010). Many factors play a significant role in drought, like extreme heat waves, low relative humidity, and rainfall frequency and distribution during the growing season (IDMP, 2022). However, low-rainfall areas are the most vulnerable spots to drought episodes primarily due to

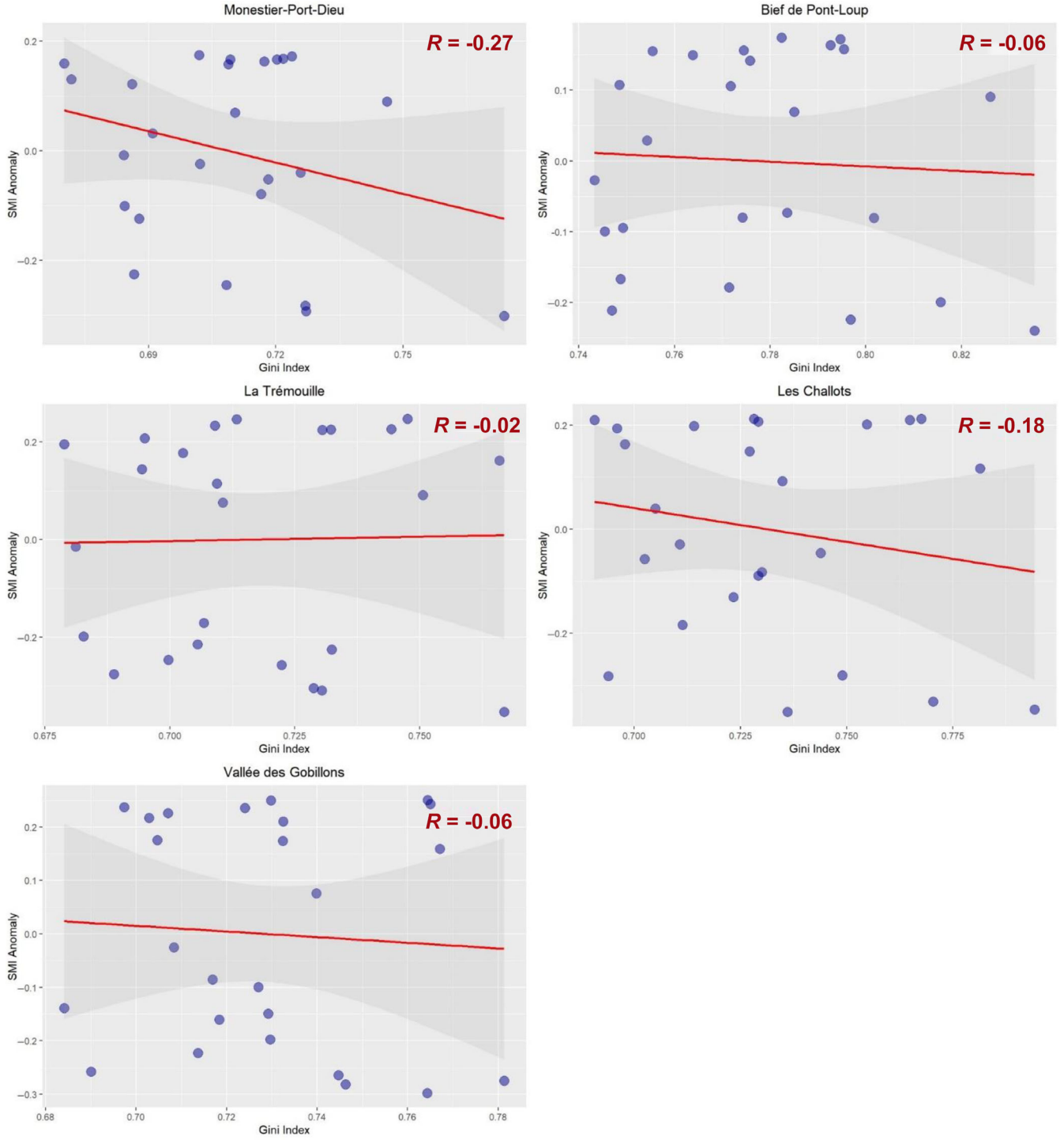

FIGURE 3 Correlation between Gini index and soil moisture index anomaly in different test areas.

reduced precipitation over an extended period (Dai, 2011).

In this context, the top drought events in Europe between 1980 and 2015 were extracted and compared with the Gini index variation, as presented in Figure 5. Drought episodes have consistently occurred alongside local peaks in the Gini index during the same year, indicating a potential association between drought and precipitation, which is in line with the findings of Wang et al. (2021) and Moazzam et al. (2022) regarding the effect of precipitation heterogeneity on the occurrence of seasonal droughts. The non-synchrony cases between drought and Gini index peaks can be explained by the fact that precipitation anomalies were not the main driver for the drought episode like the case of 1991–1992, which was a prolonged drought period across the

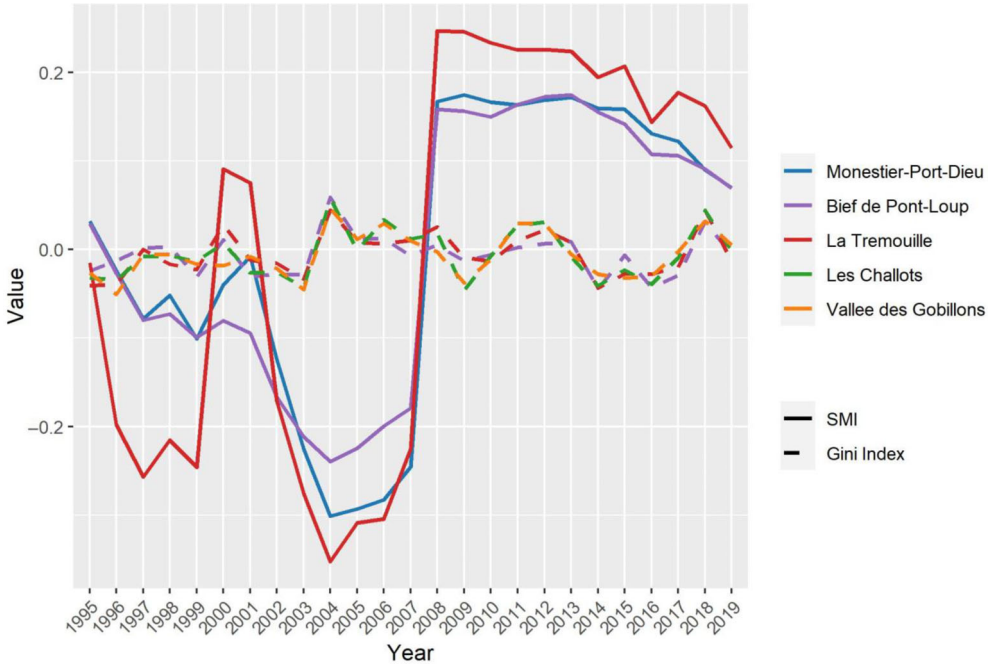

FIGURE 4 Temporal variation of soil moisture index (SMI) and Gini index anomalies between 1995 and 2019.

Mediterranean due to rain deficit in that region according to the European Drought Center report (1995). Nevertheless, it probably extended to surrounding areas, mainly Northern Europe.

Furthermore, the spatiotemporal variation of drought events has been investigated. As shown in Figure 6, the most significant drought episodes occurred in 1982, 1985, 1992, 1993, 1996–1997, 2003, 2011, and 2015, with 1996–1997 and 2003 being the most severe, followed by 2011. According to the European Drought Center, the 1996–1997 drought was characterized by meteorological shortages in the UK, followed by an ever-expanding drought in Southern Scandinavia and Northern Germany (EDC, 1997). The event began with a dry winter in 1995 and continued into 1996 and the spring of 1997, reducing available water for western Europe in the early spring. This is consistent with the Gini index anomaly map for the same period, as shown in Figure 7.

In addition, a large part of Europe was affected by another severe drought in 2003 as a consequence of rain deficits combined with elevated temperatures, causing high evapotranspiration levels that led to around ten billion Euros of agricultural losses, according to the EDO Drought News report released by the joint research center (2015). This is consistent with our results of the Gini index anomaly for the same year, which reached +0.2 across Western Europe. From January to April 2011, severe cumulated rain deficits were recorded in France and the rest of Europe, considered the driest period since 1975, according to the EDO Drought News report of 2011 (EDO-JRC, 2011). In fact, similar patterns were found in the 2011-Gini index map. Besides, the prolonged rainfall shortages in April 2015 and the temperature anomalies in July of the same period caused a severe drought that affected soil moisture content and vegetation (EDO-JRC, 2015), in consistency with the Gini index map for 2015.

For validation purposes, we have compared the patterns of Gini index anomaly in 2021 and 2022 with the occurrence of drought events in the same period. Although the 2021 spring in Europe was cooler than usual, with certain regions experiencing an early spring followed by a late frost episode that impacted agricultural productivity hence crop yields, the summer brought record-high temperatures, intense and protracted heatwaves, and flooding events, making it the "year of contrasts" for Europe between heatwaves, wildfires, and floods. The European State of the Climate (2021) report states that outside of the 10 warmest years on record, annual surface air temperatures in 2021 were only about 0.2°C higher than the average from 1991 to 2020. Indeed, this corroborates with the regional pattern found in the Gini index anomaly map of 2021, which revealed an abundance of negative anomalies that could reach −0.05 in some areas, as shown in Figure 8. In contrast to 2021, according to Toreti et al. (2022), a severe drought affected Europe since the beginning of 2022 and continues to expand in July and August 2022. The main drivers are lack of rainfall which mainly affected water resources by reducing river discharges in Europe, and combined with intense heatwaves, which led to a deficit in crop yields in May and June 2022. As a result of water resources shortages, severe impacts on the energy sector have been registered, as well as significant losses in agricultural productivity of maize, soybeans, and sunflowers fields.

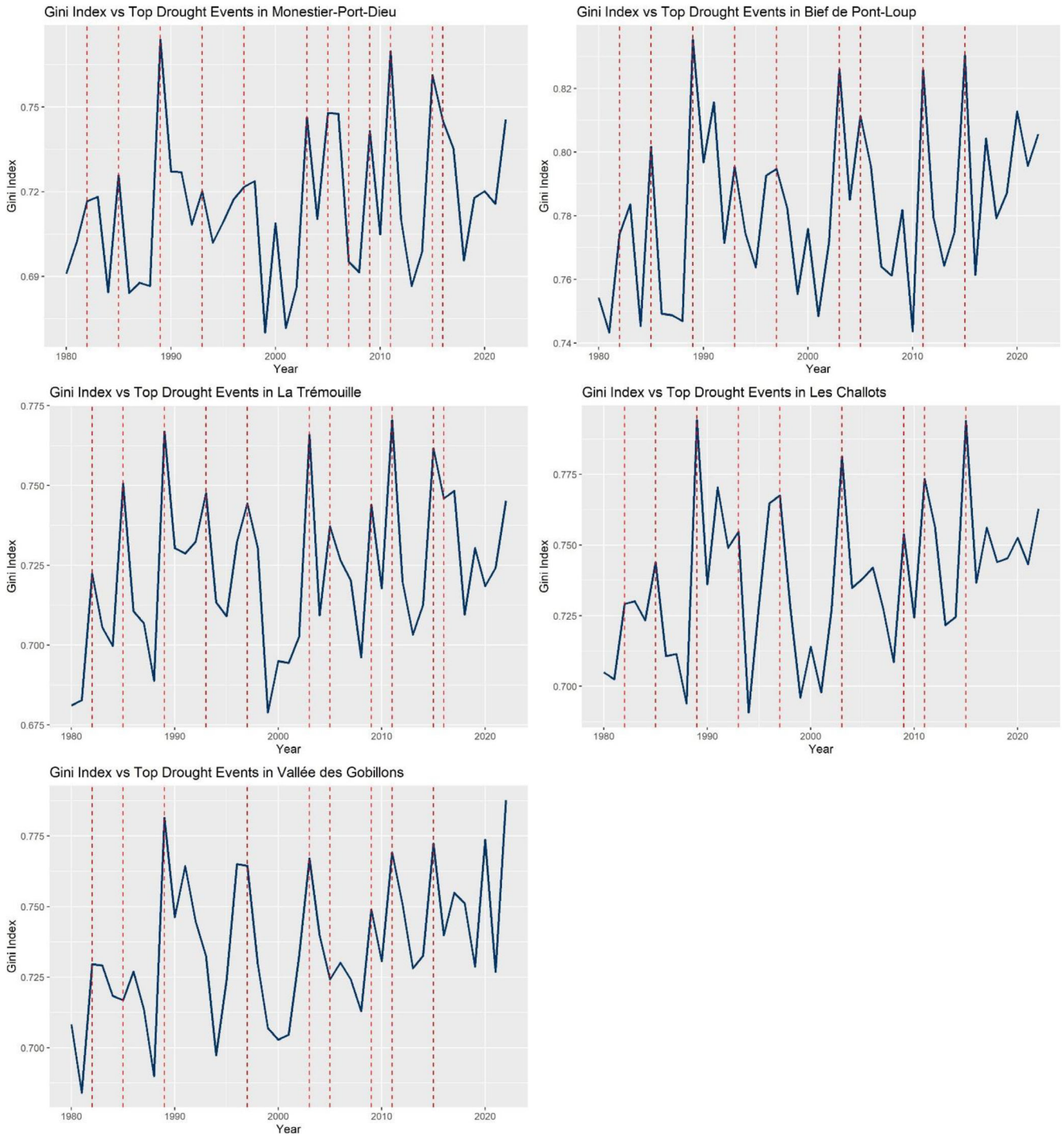

FIGURE 5 The variation of the rainfall Gini index in the test locations in synchrony with the major drought events recorded since 1980, according to the European drought observatory (EDO), where the vertical lines symbolize drought episodes.

The overall situation agrees with the spatial pattern in the Gini index anomaly map for the same year, as presented in Figure 9.

Merely, the drought scenarios explained above compared with Gini index results prove the potential of the Rainfall Gini index as a valuable drought indicator that can be considered in future studies related to drought monitoring and mapping. This can be further confirmed by Samantaray et al. (2022) regarding rainfall patterns' connection to drought characteristics. Further, Nugroho et al. (2021) revealed that precipitation anomaly is a triggering factor for drought based on a statistical analysis conducted across Indonesia using Climate Hazards Group InfraRed Precipitation with Station (CHIRPS)

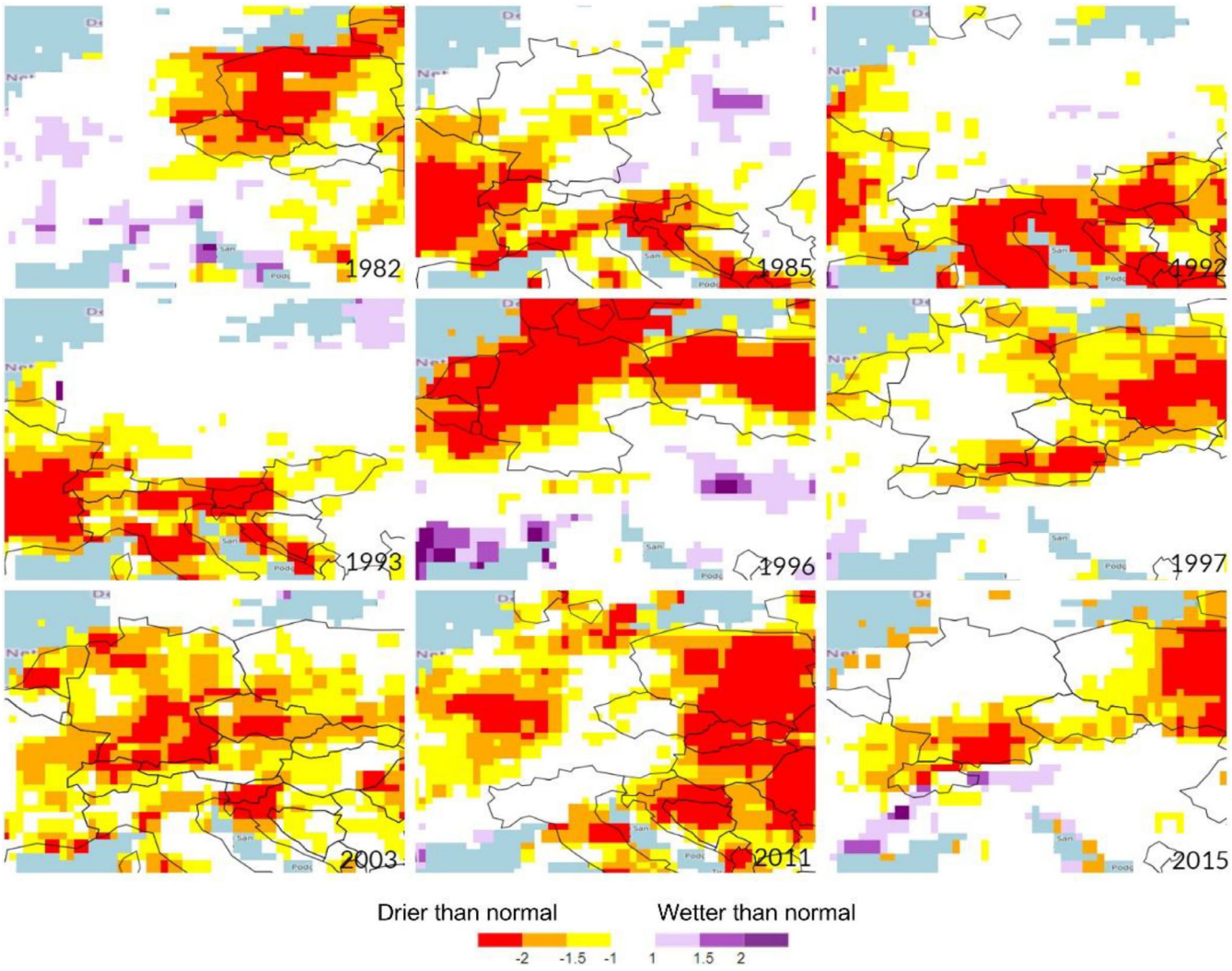

FIGURE 6 Examples of major drought events in Europe between 1980 and 2016 (EDO, 2021).

data, which corroborates with the present study regarding the present synchrony between precipitation anomaly and drought occurrence over practically the same period.

While our comparison was qualitative and did not assess the severity or magnitude of temporal changes, the synchronicity between the Gini index and drought is visually evident and firmly established. However, a statistical analysis of the relationship between these two factors would be necessary to draw conclusive evidence. This is consistent with the study of Luo et al. (2017), who found remarkably comparable results between precipitation anomalies and long-term agricultural drought episodes in California from 2012 to 2015. In a similar context, De la Barreda et al. (2020) also investigated drought episodes in the Yucatan Peninsula (Mexico) in relationship with precipitation anomalies between 1980 and 2011. The study found that drought can be regionalized using information about precipitation anomalies over time to improve drought monitoring and land management strategies in the area, which agrees with the current study's aims and findings.

It is worth noting that the relationship is not very straightforward to be outlined due to the complicated dynamics of drought and its association with multiple factors, not only rainfall but other diverse biotic and abiotic factors like temperature, soil, and vegetation. Nevertheless, this qualitative analysis reveals that the Gini index can be a valuable tool for drought monitoring and assessment while considering other influential factors. As this indicator had comparable regional and temporal patterns, it could be linked to a simultaneous occurrence of a drought season in the exact location. Many scenarios could be investigated using the Gini index as it clearly showed related patterns to drought. Future work will explore the statistical aspect of this connection and quantify drought risks and magnitude using Gini index anomaly and other related parameters like soil type, vegetation, land use and land cover, and topography.

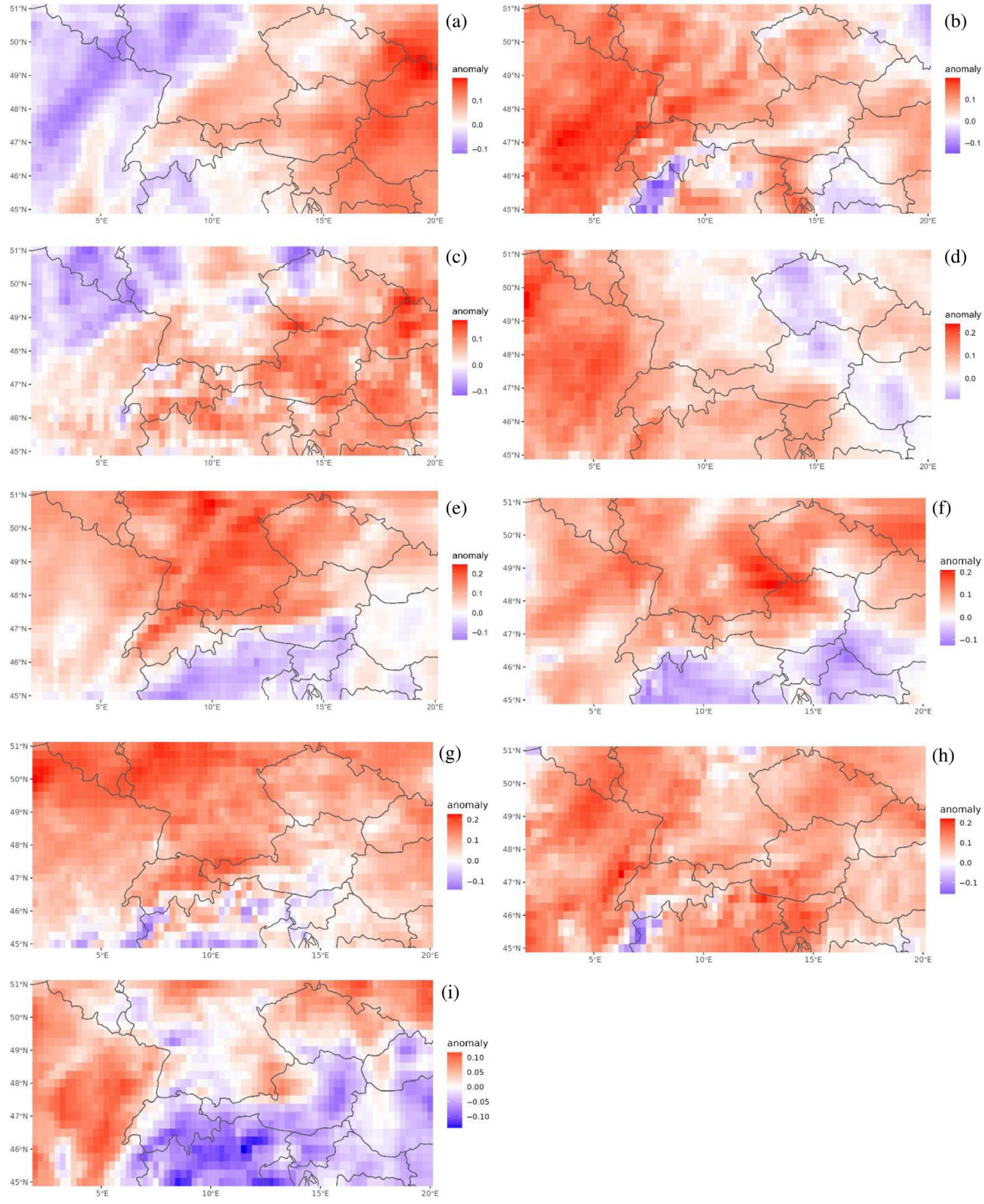

FIGURE 7 The spatiotemporal variation of the Gini index anomaly in association with the most significant drought events in Europe between 1980 and 2016: (a) 1982, (b) 1985, (c) 1992, (d) 1993, (e) 1996, (f) 1997, (g) 2003, (h) 2011, and (i) 2015.

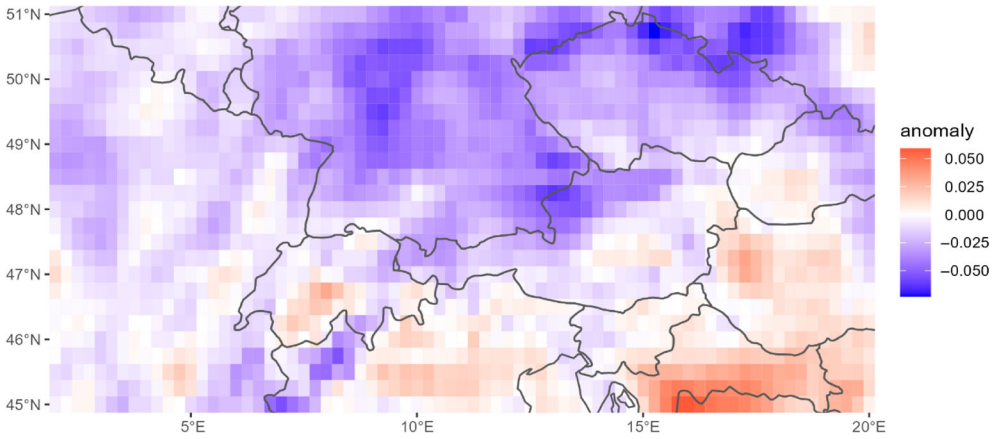

FIGURE 8 Gini index anomaly map for 2021.

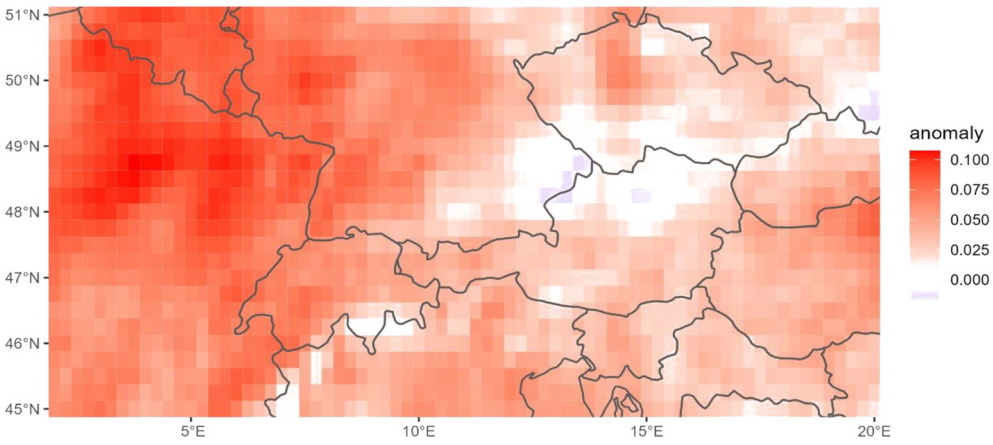

FIGURE 9 Gini index anomaly map for 2022.

4 | CONCLUSION

The results indicated that daily precipitation oscillated over time with a minimal decreasing trend from 1980 until 2022, revealed by a tau value ranging between −0.259 and −0.256 at a 5% significance level. Further, the Gini index showed an increasing trend (0.18–0.3), with an overall low negative correlation with the SMI (4 out of 5 selected locations). This suggests that each selected location had particular environmental characteristics and local climatic conditions, making it more challenging to generalize. Equally, soil moisture heavily depends on various environmental, pedogenetic, topographic, and geomorphologic features, not solely precipitation, making it more challenging to simplify interactions among various hydroclimatic components to a single variable. On the other hand, not only did the Gini index often show synchrony with drought events over time, but its spatial variation revealed similar patterns with significant drought events in Western Europe.

Although there was no statistical significance for the relationship between Gini index and SMI, comparing patterns of drought extent with Gini index showed that the Gini index can be considered a reliable drought indicator in qualitative analysis; hence can be used in parametric insurance for drought events assessment and monitoring. Future studies should focus on quantitatively establishing the statistical relationship while considering other key drivers.

This study proves that the rainfall Gini index can be used to understand drought events in Europe. The uniqueness of the research is reflected in applying it as an indicator of drought events instead of traditional indicators like the SMI, emphasizing its potential in drought monitoring and early warning systems. The increasing trend in the Gini index can be used to monitor and predict the likelihood of drought events, which can impact agriculture and food security on regional and global scales.

AUTHOR CONTRIBUTIONS

Ghada Sahbeni: Conceptualization; formal analysis; investigation; methodology; validation; visualization; writing – original draft; writing – review and editing. **Jean-Baptiste Pleynet:** Conceptualization; project administration; resources; software; supervision; validation; visualization; writing – review and editing. **Konrad Jarocki:** Conceptualization; data curation; methodology;

resources; software; validation; writing – review and editing.

ACKNOWLEDGEMENTS

This research was proposed by IBISA SA (https://ibisa.network) and supported by its resources. The APCs are covered by Eötvös Loránd University. ERA5 data are acquired from the ECMWF. SMI and Top Drought data are downloaded from the European Drought Observatory (EDO).

CONFLICT OF INTEREST STATEMENT

The authors declare no competing interests.

DATA AVAILABILITY STATEMENT

IBISA SA can provide the datasets and R scripts generated during this research upon a reasonable request.

ORCID

Ghada Sahbeni https://orcid.org/0000-0001-8595-3043

REFERENCES

Abed-Elmdoust, A., Miri, M. & Singh, A. (2016) Reorganization of river networks under changing spatiotemporal precipitation patterns: an optimal channel network approach. *Water Resources Research*, 52, 8845–8860 Available from: https://doi.org/10.1002/2015WR018391

Ali, A., Lebel, T. & Amani, A. (2003) Invariance in the spatial structure of Sahelian rain fields at climatological scales. *Journal of Hydrometeorology*, 4(6), 996–1011 Available from: https://doi.org/10.1175/1525-7541(2003)004%3C0996:IITSSO%3E2.0.CO;2

Alimonti, G., Mariani, L., Prodi, F. & Ricci, R.A. (2022) A critical assessment of extreme events trends in times of global warming. *European Physical Journal-Plus*, 137, 112 Available from: https://doi.org/10.1140/epjp/s13360-021-02243-9

Broberg, M.P. (2019) Parametric loss and damage insurance schemes as a means to enhance climate change resilience in developing countries. *Climate Policy*, 20, 693–703 Available from: https://doi.org/10.1080/14693062.2019.1641461

Cammalleri, C., Micale, F. & Vogt, J. (2016) A novel soil moisture-based drought severity index (DSI) combining water deficit magnitude and frequency. *Hydrological Processes*, 30(2), 289–301 JRC96439. Available from: https://hess.copernicus.org/articles/21/6329/2017/

Carrão, H., Naumann, G. & Barbosa, P.M. (2016) Mapping global patterns of drought risk: an empirical framework based on sub-national estimates of hazard, exposure, and vulnerability. *Global Environmental Change*, 39, 108–124 Available from: https://doi.org/10.1016/j.gloenvcha.2016.04.012

Ceriani, L. & Verme, P. (2012) The origins of the Gini index: extracts from variabilità e mutabilità (1912) by Corrado Gini. *The Journal of Economic Inequality*, 10, 421–443 Available from: https://doi.org/10.1007/s10888-011-9188-x

Climate Change Service (C3S). (2022) Climate datasets—climate reanalysis. Available from: https://climate.copernicus.eu/climate-reanalysis

Climate Data Guide. (2022) ERA5 atmospheric reanalysis. Available from: https://climatedataguide.ucar.edu/climate-data/era5-atmospheric-reanalysis

Coughlan de Perez, E., van Aalst, M., Choularton, R., van den Hurk, B., Mason, S., Nissan, H. et al. (2019) From rain to famine: assessing the utility of rainfall observations and seasonal forecasts to anticipate food insecurity in East Africa. *Food Security*, 11, 57–68 Available from: https://doi.org/10.1007/s12571-018-00885-9

Dai, A. (2011) Drought under global warming: a review. *Wiley Interdisciplinary Reviews: Climate Change*, 2, 45–65 Available from: https://doi.org/10.1002/wcc.81

Dai, A. & Trenberth, K.E. (2004) The diurnal cycle and depth of the atmospheric boundary layer over land. *Journal of Climate*, 17(19), 4067–4086 Available from: https://doi.org/10.1175/JCLI3292.1

De la Barreda, B., Metcalfe, S.E. & Boyd, D.S. (2020) Precipitation regionalization, anomalies, and drought occurrence in the Yucatan Peninsula, Mexico. *International Journal of Climatology*, 40, 4541–4555 Available from: https://doi.org/10.1002/joc.6474

De Roo, A., Wesseling, C. & Van Deursen, W. (2000) Physically based river basin modelling within a GIS: the LISFLOOD model. *Hydrological Processes*, 14, 1981–1992 Available from: https://doi.org/10.1002/1099-1085(20000815/30)14:11/12<1981::AID-HYP49>3.0.CO;2-F

Duan, W., Zou, S., Christidis, N., Schaller, N., Chen, Y., Sahu, N. et al. (2022) Changes in temporal inequality of precipitation extremes over China due to anthropogenic forcings. *NPJ Climate and Atmospheric Science*, 5, 33 Available from: https://doi.org/10.1038/s41612-022-00255-5

ECMWF. (2022) ERA5: data documentation. Available from: https://confluence.ecmwf.int/display/CKB/ERA5%3A+data+documentation

EDC. (1995) Major drought events–drought of 1991–1995. Available from: https://www.geo.uio.no/edc/droughtdb/edr/DroughtEvents/_1991_Event.php

EDC. (1997) Major drought events–drought of 1995–1996. Available from: https://www.geo.uio.no/edc/droughtdb/edr/DroughtEvents/1996_Event.php

Edgar, L.A., Fedo, C.M., Gupta, S., Banham, S.G., Fraeman, A.A., Grotzinger, J.P. et al. (2020) A lacustrine paleoenvironment recorded at Vera Rubin Ridge, Gale crater: overview of the sedimentology and stratigraphy observed by the Mars science laboratory curiosity rover. *Journal of Geophysical Research: Planets*, 125(3), e2019JE006307 Available from: https://doi.org/10.1029/2019JE006307

EDO. (2021) Standardized Precipitation Index (SPI). Available from: https://edo.jrc.ec.europa.eu/documents/factsheets/factsheet_spi.pdf

EDO-JRC. (2011) Drought news in Europe: situation in April 2011: short Analysis of data from the European Drought Observatory (EDO). Available from: https://edo.jrc.ec.europa.eu/edov2/php/index.php?id=1000

EDO-JRC. (2015) Drought news August 2015: EDO Combined Drought Indicator (CDI)—situation on 31 July 2015. Available from: https://edo.jrc.ec.europa.eu/edov2/php/index.php?id=1000

EEA. (2017) Report: indicator assessment: mean precipitation. Available from: https://www.eea.europa.eu/data-and-maps/indicators/european-precipitation-2/assessment

EDO. (2021) EDO indicator factsheet—soil moisture anomaly (SMA). Available from: https://edo.jrc.ec.europa.eu/gdo/php/index.php?id=2112

European State of the Climate 2021. (2021) Copernicus climate change service, full report. Available from: https://doi.org/10.21957/9d7g-hn83

Gastwirth, J.L. (1972) The estimation of the Lorenz curve and Gini index. *The Review of Economics and Statistics*, 54(3), 306–316 Available from: https://doi.org/10.2307/1937992

Ghorbani, M., Mahmoud Alilou, S., Javidan, S. & Naganna, S.R. (2021) Assessment of spatio-temporal variability of rainfall and mean air temperature over Ardabil province, Iran. SN. *Applied Sciences*, 3, 728. Available from: https://doi.org/10.1007/s42452-021-04698-y–710.

Grillakis, M.G. (2019) Increase in severe and extreme soil moisture droughts for Europe under climate change. *The Science of the Total Environment*, 660(10), 1245–1255 Available from: https://doi.org/10.1016/j.scitotenv.2019.01.001

Hersbach, H., Bell, B., Berrisford, P., Dahlgren, P., Horányi, A., Muñoz-Sabater, J. et al. (2020) The ERA5 Global Reanalysis: achieving a detailed record of the climate and weather for the past 70 years. *EGU2020-10375*, 1–24 Available from: https://doi.org/10.5194/egusphere-egu2020-10375

Hersbach, H., Bell, B., Berrisford, P., Hirahara, S., Horányi, A., Muñoz-Sabater, J. et al. (2020) The ERA5 global reanalysis. *Quarterly Journal of the Royal Meteorological Society*, 146, 1999–2049 Available from: https://doi.org/10.1002/qj.3803

Hersbach, H., Bell, B., Berrisford, P., Horányi, A.J.M.S., Sabater, J. M., Nicolas, J. et al. (2019) Global reanalysis: goodbye ERA-Interim, hello ERA5. *ECMWF Newsletter*, 159, 17–24 Available from: https://doi.org/10.21957/vf291hehd7

Huo, R., Li, L., Chen, H., Xu, C., Chen, J. & Guo, S. (2021) Extreme precipitation changes in Europe from the last millennium to the end of the twenty-first century. *Journal of Climate*, 34(2), 567–588. Available from: https://journals.ametsoc.org/view/journals/clim/34/2/JCLI-D-19-0879.1.xml

IDMP. (2022) Drought and Water Scarcity. WMO No. 1284. Global Water Partnership, Stockholm, Sweden and World Meteorological Organization, Geneva, Switzerland. Available from: https://library.wmo.int/doc_num.php?explnum_id=11108

IPCC. (2022) Summary for policymakers. In: Pörtner, H.O., Roberts, D.C., Poloczanska, E.S., Mintenbeck, K., Tignor, M., Alegría, A. et al. (Eds.) *Climate change 2022: impacts, adaptation, and vulnerability. Contribution of working group II to the sixth assessment report of the intergovernmental panel on climate change*. Cambridge, UK and New York, NY, USA: Cambridge University Press. Available from: https://www.ipcc.ch/report/ar6/wg2/

Jackson, T.J., Chen, D., Cosh, M.H., Li, F., Anderson, M.C., Walthall, C.L. et al. (2010) Vegetation water content mapping using Landsat data derived normalized difference water index for corn and soybeans. *Remote Sensing of Environment*, 114(11), 2169–2177 Available from: https://doi.org/10.1016/j.rse.2010.05.010

Karmeshu, N. (2012) Trend detection in annual temperature & precipitation using the Mann Kendall Test—a case study to assess climate change on select states in the Northeastern United States. Available from: https://repository.upenn.edu/cgi/viewcontent.cgi?article=1045&context=mes_capstones

Khambhammettu, P. (2005) Mann-Kendall analysis. HydroGeoLogic, Inc.—OU-1 2004 Annual Groundwater Monitoring Report—Former Fort Ord, California. Available from: https://www.statisticshowto.com/wp-content/uploads/2016/08/Mann-Kendall-Analysis-1.pdf

Laguardia, G. & Niemeyer, S. (2008) On the comparison between the LISFLOOD modeled and the ERS/SCAT derived soil moisture estimates. *Hydrology and Earth System Sciences*, 12, 1339–1351 Available from: https://doi.org/10.5194/hess-12-1339-2008

Liang, L., Peng, S., Sun, J., Chen, L. & Cao, Y. (2010) Estimation of annual potential evapotranspiration at regional scale based on the effect of moisture on soil respiration. *Ecological Modeling*, 221, 2668–2674 Available from: https://doi.org/10.1016/j.ecolmodel.2010.08.010

Luo, L., Apps, D., Arcand, S., Xu, H., Pan, M. & Hoerling, M.P. (2017) Contribution of temperature and precipitation anomalies to the California drought during 2012–2015. *Geophysical Research Letters*, 44, 3184–3192 Available from: https://doi.org/10.1002/2016GL072027

Masaki, Y., Hanasaki, N., Takahashi, K. & Hijioka, Y. (2014) Global-scale analysis on future changes in flow regimes using Gini and Lorenz asymmetry coefficients. *Water Resources Research*, 50(5), 4054–4078 Available from: https://doi.org/10.1002/2013WR014266

Masson-Delmotte, V., Raffalli-Delerce, G., Danis, P., Yiou, P., Stiévenard, M., Guibal, F. et al. (2005) Changes in European precipitation seasonality and in drought frequencies revealed by a four-century-long tree-ring isotopic record from Brittany, western France. *Climate Dynamics*, 24, 57–69 Available from: https://doi.org/10.1007/s00382-004-0458-1

McCabe, G.J. & Wolock, D.M. (2013) Temporal and spatial variability of global water balance. *Climatic Change*, 120, 375–387 Available from: https://doi.org/10.1007/s10584-013-0798-0

McKee, T.B., Doesken, N.J. & Kleist, J. (1993) The relationship of drought frequency and duration to time scale. In: *Proceedings of the Eighth Conference on Applied Climatology, Anaheim, California, 17–22 January 1993*. Boston: American Meteorological Society, pp. 179–184 Available from: https://www.droughtmanagement.info/literature/AMS_Relationship_Drought_Frequency_Duration_Time_Scales_1993.pdf

Meals, D.W., Spooner, J., Dressing, S.A. & Harcum, J.B. (2011) Statistical analysis for monotonic trends, Tech Notes 6, November 2011. Developed for U.S. Environmental Protection Agency by Tetra Tech, Inc., Fairfax, VA, 23. Available from: https://www.epa.gov/polluted-runoff-nonpoint-source-pollution/nonpoint-source-monitoringtechnical-notes

Meng, X., Li, R., Luan, L., Lyu, S., Zhang, T., Ao, Y. et al. (2018) Detecting hydrological consistency between soil moisture and precipitation and changes of soil moisture in summer over the Tibetan plateau. *Climate Dynamics*, 51, 4157–4168 Available from: https://doi.org/10.1007/s00382-017-3646-5

Mishra, A.K. & Singh, V.P. (2010) A review of drought concepts. *Journal of Hydrology*, 391, 202–216 Available from: https://doi.org/10.1016/j.jhydrol.2010.07.012

Moazzam, M.F.U., Rahman, G., Munawar, S., Tariq, A., Safdar, Q. & Lee, B.-G. (2022) Trends of rainfall variability and drought monitoring using standardized precipitation index in a scarcely Gauged Basin of northern Pakistan. *Water*, 14(7), 1132 MDPI AG. Available from: https://doi.org/10.3390/w14071132

Monjo, R. & Martín-Vide, J. (2016) Daily precipitation concentration around the world according to several indices. *International Journal of Climatology*, 36(11), 3828–3838 Available from: https://doi.org/10.1002/joc.4596

Monteleone, B., Martina, M. & Bonaccorso, B. (2020) A parametric insurance framework based on remote-sensing observations to mitigate drought impacts through risk financing. *EGU General-Assembly*, EGU2020-11283. Available from: https://doi.org/10.5194/egusphere-egu2020-11283

Nugroho, J.T., Nurfitriani, D., Suwarsono Chulafak, G.A., Manalu, R. & Harini, S. (2021) Rainfall anomalies assessment during drought episodes of 2015 in Indonesia using CHIRPS data. *IOP Conference Series: Earth and Environmental Science*, 739, 012044 Available from: https://doi.org/10.1088/1755-1315/739/1/012044

Radu, N. & Alexandru, F. (2022) Parametric insurance—a possible and necessary solution to insure the earthquake risk of Romania. *Risks*, 10(3), 59 Available from: https://doi.org/10.3390/risks10030059

Rajah, K., O'Leary, T.J., Turner, A.R., Petrakis, G., Leonard, M. & Westra, S. (2014) Changes to the temporal distribution of daily precipitation. *Geophysical Research Letters*, 41, 8887–8894 Available from: https://doi.org/10.1002/2014GL062156

Saha, A., Patil, M., Goyal, V.C. & Rathore, D.S. (2018) Assessment and impact of soil moisture index in agricultural drought estimation using remote sensing and GIS techniques. *Proceedings*, 7(1), 2 Available from: https://doi.org/10.3390/ecws-3-05802

Samantaray, A.K., Ramadas, M. & Panda, R.K. (2022) Changes in drought characteristics based on rainfall pattern drought index and the CMIP6 multi-model ensemble. *Agricultural Water Management*, 266, 107568 Available from: https://doi.org/10.1016/j.agwat.2022.107568

Sangüesa, C., Pizarro, R., Ibañez, A., Pino, J., Rivera, D., García-Chevesich, P. et al. (2018) Spatial and temporal analysis of rainfall concentration using the Gini index and PCI. *Water*, 10(2), 112 Available from: https://doi.org/10.3390/w10020112

Sarker, S., Veremyev, A., Boginski, V. & Singh, A. (2019) Critical nodes in river networks. *Scientific Reports*, 9, 11178 Available from: https://doi.org/10.1038/s41598-019-47292-4

Schwank, M., Albergel, C., Calvet, J.C., Zhang, L. & Balsamo, G. (2013) The SMOS soil moisture retrieval: comparison within situ measurements and other satellite data sets. *Remote Sensing of Environment*, 131, 149–162 Available from: https://doi.org/10.1016/j.rse.2012.12.005

Sehler, R.C., Li, J., Reager, J.T. & Ye, H. (2019) Investigating relationship between soil moisture and precipitation globally using remote sensing observations. *Journal of Contemporary Water Research & Education*, 168, 106–118 Available from: https://doi.org/10.1111/j.1936-704X.2019.03324.x

Seneviratne, S.I., Zhang, X., Adnan, M., Badi, W., Dereczynski, C., Di Luca, A. et al. (2021) Weather and climate extreme events in a changing climate. In: Masson-Delmotte, V., Zhai, P., Pirani, A., Connors, S.L., Péan, C., Berger, S. et al. (Eds.) *Climate change 2021: the physical science basis. Contribution of working group I to the sixth assessment report of the intergovernmental panel on climate change*. Cambridge, United Kingdom and New York, NY, USA: Cambridge University Press, pp. 1513–1766 Available from: https://doi.org/10.1017/9781009157896.013

Singh, D., Seager, R., Cook, B.I., Cane, M., Ting, M., Cook, E. et al. (2018) Climate and the global famine of 1876–78. *Journal of Climate*, 31(23), 9445–9467 Available from: https://journals.ametsoc.org/view/journals/clim/31/23/jcli-d-18-0159.1.xml

Soltani, M., Laux, P., Kunstmann, H., Stan, K., Sohrabi, M.M., Molanejad, M. et al. (2016) Assessment of climate variations in temperature and precipitation extreme events over Iran. *Theoretical and Applied Climatology*, 126, 775–795 Available from: https://doi.org/10.1007/s00704-015-1609-5

Song, X., Song, S., Sun, W., Mu, X., Wang, S., Li, J. et al. (2015) Recent changes in extreme precipitation and drought over the Songhua River Basin, China, during 1960-2013. *Atmospheric Research*, 157, 137–152 Available from: https://doi.org/10.1016/j.atmosres.2015.01.022

Spinoni, J., Barbosa, P.M., de Jager, A., McCormick, N., Naumann, G., Vogt, J.V. et al. (2019) A new global database of meteorological drought events from 1951 to 2016. *Journal of Hydrology: Regional Studies*, 22, 100593 Available from: https://doi.org/10.1016/j.ejrh.2019.100593

Toreti, A., Bavera, D., Acosta Navarro, J., Cammalleri, C., de Jager, A., Di Ciollo, C. et al. (2022) *Drought in Europe August 2022*. Luxembourg: Publications Office of the European Union. Available from: https://data.europa.eu/doi/10.2760/264241

Van Der Knijff, J.M., Younis, J. & De Roo, A.P.J. (2010) LISFLOOD: a GIS-based distributed model for river basin scale water balance and flood simulation. *International Journal of Geographical Information Science*, 24, 189–212 Available from: https://doi.org/10.1080/13658810802549154

Vicente-Serrano, S.M., Beguería, S. & López-Moreno, J.I. (2010) A multiscalar drought index sensitive to global warming: the standardized precipitation evapotranspiration index. *Journal of Climate*, 23(7), 1696–1718 Available from: https://journals.ametsoc.org/view/journals/clim/23/7/2009jcli2909.1.xm

Voskresenskaya, E., Vyshkvarkova, E. & Polonskii, A. (2013) Global climate change and associated precipitation inequality over Ukraine. *Geophysical Research Abstracts*, 15, EGU2013–EGU11341, EGU General Assembly 2013 Available from: https://meetingorganizer.copernicus.org/EGU2013/EGU2013-11341.pdf

Wang, F., Shao, W., Yu, H., Kan, G., He, X., Zhang, D. et al. (2020) Re-evaluation of the power of the Mann-Kendall test for detecting monotonic trends in hydrometeorological time series. *Frontiers in Earth Science*, 8, 14 Available from: https://doi.org/10.3389/feart.2020.00014

Wang, S., Zhang, Q., Wang, J., Liu, Y. & Zhang, Y. (2021) Relationship between drought and precipitation heterogeneity: an analysis across rain-fed agricultural regions in eastern Gansu, China. *Atmosphere*, 12(10), 1274 MDPI AG. Available from: https://doi.org/10.3390/atmos12101274

Wang, Y., Yang, J., Chen, Y., de Maeyer, P., Li, Z. & Duan, W. (2018) Detecting the causal effect of soil moisture on precipitation using convergent cross mapping. *Scientific Reports*, 8, 12171 Available from: https://doi.org/10.1038/s41598-018-30669-2

Zaveri, E.D., Russ, J.D. & Damania, R. (2020) Rainfall anomalies are a significant driver of cropland expansion. *Proceedings of the National Academy of Sciences*, 117, 10225–10233 Available from: https://doi.org/10.1073/pnas.1910719117

Zeder, J. & Fischer, E.M. (2020) Observed extreme precipitation trends and scaling in Central Europe. *Weather and Climate Extremes*, 29, 100266 Available from: https://doi.org/10.1016/j.wace.2020.100266

Zhang, Y., Gong, J., Sun, K., Yin, J. & Chen, X. (2017) Estimation of soil moisture index using multi-temporal Sentinel-1 images over Poyang lake ungauged zone. *Remote Sensing*, 10(2), 12 MDPI AG. Available from: https://doi.org/10.3390/rs10010012

How to cite this article: Sahbeni, G., Pleynet, J. B., & Jarocki, K. (2023). A spatiotemporal analysis of precipitation anomalies using rainfall Gini index between 1980 and 2022. *Atmospheric Science Letters*, e1161. https://doi.org/10.1002/asl.1161